

Ohmic Electron Injection into Organic Semiconductors by Solution-Processed and Evaporated Organic Interlayers

David Trieb, Paul W.M. Blom, and Gert-Jan A.H. Wetzelaer*

Efficient electron injection from an electrode into an organic semiconductor remains a problem to solve for efficient organic semiconductor devices. In this work, a general method is presented to form an ohmic electron contact by inserting a thin organic interlayer between the metal electrode and the organic semiconductor. It is demonstrated that inserting an interlayer of a few nanometers of an organic semiconductor with a lower electron affinity than the transport material can improve the injected electron current by over three orders of magnitude. The electron current becomes space-charge limited, demonstrating that the interlayer-enhanced contact is ohmic. The ohmic-contact formation by inserting a thin interlayer is ascribed to the elimination of barrier formation as a result of direct contact between the metal and organic semiconductor. Additionally, it is demonstrated that it is possible to achieve solution processing of such interlayers on top of organic semiconductors. The method is generalized for different interlayer materials as well as for different organic semiconductors, providing a general method for ohmic electron injection in organic devices.

to prevent charge-injection barriers.^[2] As the injected current scales exponentially with the injection barrier, it is important that the barriers be minimized. Ideally, an ohmic contact is formed, corresponding to barrierless charge injection from the electrode into the organic semiconductor.

To achieve ohmic contacts on organic semiconductors, several methods have been developed. To achieve low work-function contacts for electron injection, typically metals with a low work function such as barium or calcium are applied.^[3] Additionally, thin interlayers of metal salts like LiF or Cs₂CO₃ are commonly used.^[4] For hole injection, transition metal oxides, such as MoO₃, are often used as an inorganic injection layer, because of their extremely high work function of up to 6.9 eV.^[5,6] However, despite their very high work function, it was recently found that the contacts formed with these


metal oxides are non-ohmic. The unexpected hole injection barrier could be eliminated by using thin (3–5 nm) tunneling interlayers of organic semiconductors with a high ionization energy.^[7] These interlayers act as a spacer layer, preventing barrier formation upon direct contact between the electrode and the organic semiconductor due to electrostatic interactions. The high ionization energy of the interlayer allows the Fermi level of the metal to align with the ionization energy of the semiconductor, resulting in an ohmic contact.

Since a hole-injection barrier between MoO₃ and organic semiconductors was found despite the more than sufficiently high work function of the MoO₃ electrode, this raises concerns about the analogous case of electron injection from low work-function contacts. Indeed, for the high-mobility electron-transporting polymer poly((*N,N'*-bis(2-octyldodecyl)naphthalene-1,4,5,8-bis(dicarboxoimide)-2,6-diyl)-alt-5,5'-(2,2'-bithiophene)) [PNDI(2OD)-2T], Steyrlleuthner et al. found that ohmic electron injection could not be achieved, despite the use of a wide range of electrode materials with different work functions.^[8] Intriguingly, the electron affinity of PNDI(2OD)-2T is rather high at 3.8 eV, which should in principle be easily accessible for electron injection from low work-function metals. As such, it seems that the formation of ohmic electron contacts is not straightforward, similar to the recent observations for the formation of ohmic hole contacts.^[6] Multiple reasons have been discussed for the formation of charge-injection barriers between metals and organic semiconductors, such as chemical reactions at the interface leading to Fermi-level pinning states.^[9] In addition,

1. Introduction

Organic semiconductors are currently investigated for their use in optoelectronic devices, such as organic light-emitting diodes (OLEDs), organic photovoltaic cells (OPV), and organic field-effect transistors (OFETs).^[1] An attractive feature of organic semiconductors is their solubility in organic solvents, enabling the fabrication of optoelectronic devices by a facile and cost-effective solution process. For the efficient operation of such devices, it is of great importance that the organic semiconductor layers are contacted with the right electrodes. For efficient charge injection, the work function of the electrode has to match the ionization energy (for hole injection) or the electron affinity (for electron injection) of the organic semiconductor,

D. Trieb, P. W.M. Blom, G.-J. A.H. Wetzelaer
 Molecular Electronics
 Max Planck Institute for Polymer Research
 Ackermannweg 10, 55128 Mainz, Germany
 E-mail: wetzelaer@mpip-mainz.mpg.de

 The ORCID identification number(s) for the author(s) of this article can be found under <https://doi.org/10.1002/admi.202202424>.

© 2023 The Authors. Advanced Materials Interfaces published by Wiley-VCH GmbH. This is an open access article under the terms of the Creative Commons Attribution License, which permits use, distribution and reproduction in any medium, provided the original work is properly cited.

DOI: 10.1002/admi.202202424

the overlap between metallic states and molecular levels gives rise to broadening of the latter, leading to an induced density of interface states, to which the Fermi level is pinned.^[10] Damage to the organic semiconductor top interface may also occur when a metal is evaporated on top, potentially leading to barrier formation.^[2] For hole injection from metal oxides, the image potential due to a dielectric contrast at the interface was associated with barrier formation, which is also generally present at metal-organic interfaces.^[6]

For hole injection, the use of thin organic interlayers could solve the problem of barrier formation.^[6] As a practical demonstration of the use of tunneling interlayers to form ohmic contacts, a highly efficient single-layer OLED was fabricated, using a C₆₀ interlayer for hole injection and a 2,2',2''-(1,3,5-benzinetriyl)-tris(1-phenyl-1-H-benzimidazole) (TPBi) interlayer for electron injection.^[11] As a result of the formed ohmic contacts, a high external quantum efficiency of 19% was obtained despite the absence of transport and blocking layers, and an extremely low-operating voltage could be achieved due to the absence of injection barriers. These results show promise for efficient electron injection by using thin interlayers. As a second example of the use of such an injection strategy, tunneling interlayers have been shown to enhance the hole injection in OFETs.^[12]

Here, we demonstrate that ohmic electron contacts can be formed by using thin interlayers of organic semiconductors with a low electron affinity. Moreover, it is shown that these interlayers can be processed from solution, without compromising charge injection. Several interlayer materials are used for efficient electron injection from an aluminum electrode into the polymer PNDI(2OD)-2T and the non-fullerene acceptor IT-4F. These results highlight the potential of using tunneling interlayers in solution-processed organic devices.

2. Results and Discussion

To investigate the electron injection in the presence of a thin-tunneling interlayer, we have fabricated electron-only devices as displayed schematically in **Figure 1a**. The devices are based on the polymer PNDI(2OD)-2T, of which the molecular structure is shown in **Figure 1c**. The polymer has a high electron mobility and finds applications in *n*-type transistors and organic solar cells.^[13] As trap-free electron transport has been observed for this polymer, the formation of an ohmic electron contact should result in a space-charge-limited current, rendering this polymer ideal for investigating electron injection.^[14]

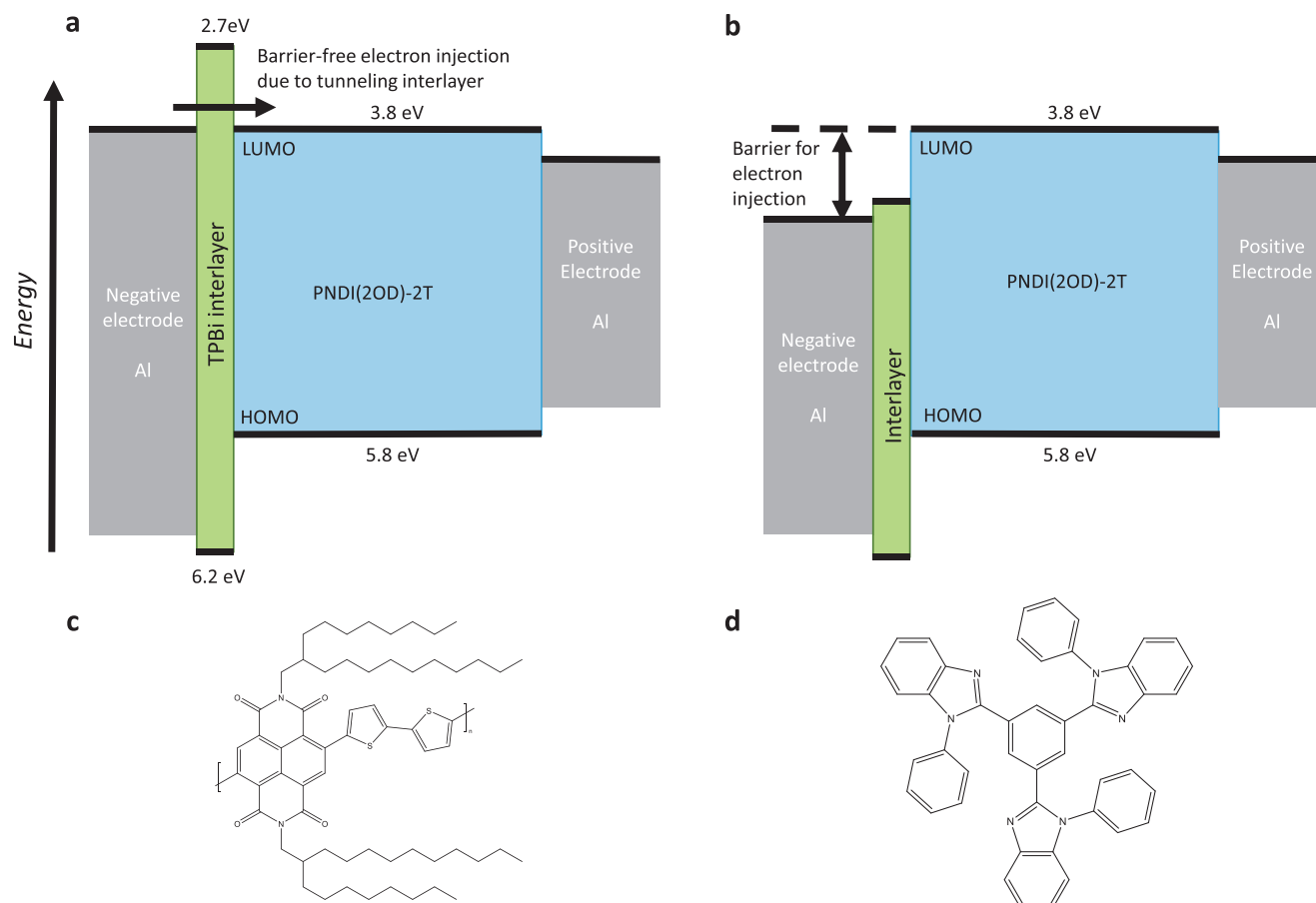


Figure 1. a) Schematic energy band diagram showing Fermi-level alignment between the electrode and the LUMO of PNDI(2OD)-2T, due to a TPBi interlayer. b) Schematic energy band diagram of a device with an interlayer with a deeper LUMO than PNDI(2OD)-2T, leading to an offset between the electrode Fermi level and the LUMO of PNDI(2OD)-2T. c) Molecular structure of the organic semiconductor PNDI(2OD)-2T. d) Molecular structure of the interlayer material TPBi.

Moreover, as observed by Steyrlleuthner et al., ohmic electron injection could not be achieved with the conventional method of using low work-function electrodes, despite investigating a wide range of injection layers.^[8] In our electron-only devices, we chose TPBi for the interlayer material, situated between the polymer layer and the aluminum top electrode. Usually, TPBi is used as an electron-transport material in organic semiconductor devices. The reason we chose TPBi for the interlayer material is the large energy offset between the lowest unoccupied molecular orbital (LUMO) of PNDI(2OD)-2T and TPBi of 1.1 eV. This is analogous to the interlayer requirement for improving hole injection, for which interlayers with a high ionization energy are required. The work function of the aluminum top electrode is not sufficient for direct electron injection into the LUMO of TPBi. Instead, the TPBi interlayer prevents direct contact between the metal and the polymer and the associated barrier formation upon contact, while the high LUMO of TPBi ensures that the Fermi level of aluminum can align with the LUMO of PNDI(2OD)-2T. The Fermi-level alignment then results in an ohmic contact where charges are transferred from the electrode, through the interlayer, into the polymer. An interlayer with too deep a LUMO (Figure 1b), however, would result in Fermi-level pinning of Al below the LUMO of the interlayer, which results in misalignment of the electrode Fermi level with the LUMO of the polymer. Similarly, the work function of the used metal electrode should be at least as low as the electron affinity of the organic semiconductor, to ensure Fermi-level alignment, analogous to the case for hole injection.^[7]

To investigate the electron-injection properties, we fabricated three types of electron-only devices: one without interlayer, one with an evaporated interlayer, and one with a solution-processed interlayer. The interlayers were deposited on top of the PNDI(2OD)-2T layer. The solution-processed interlayer was spin coated from an ethanol solution, as ethanol does not affect the layer of the PNDI(2OD)-2T, as observed from atomic force microscopy (AFM) measurements (Figure S1, Supporting Information). Details on the solution preparation and the spin-coating procedure are provided in the Experimental Section. The thickness of the interlayer in the devices was 4 nm for both deposition methods. The current density (J) versus voltage (V) characteristics of these devices are shown in Figure 2. Upon insertion of a TPBi interlayer between the polymer and the top electrode, a substantial increase of the electron current density in forward bias is visible in Figure 2, where forward bias corresponds to injection from the aluminum top electrode. At 4 V, an increase in current density of about three orders of magnitude is observed, independent of the deposition method of the interlayer. These observations indicate that the electron injection is clearly enhanced by the addition of a tunneling interlayer, and, importantly, that the interlayer can also be processed from solution, without loss of function.

To further investigate the mechanism of electron injection, we have also fabricated electron-only devices with a Ba (5 nm) and LiF (1 nm) interlayer, of which the J - V characteristics are displayed in Figure 2. It is observed that the current injected from these conventionally used interlayers is limited by the presence of a charge injection barrier. This is further confirmed when studying the activation energy of the injected current, which is larger in the absence of a TPBi interlayer, also pointing toward

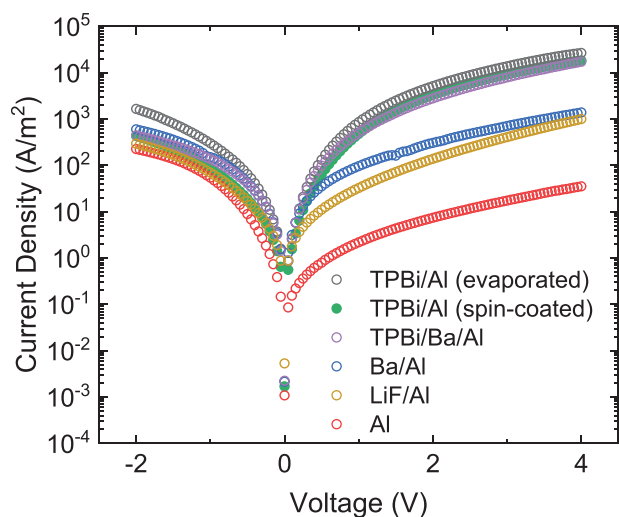


Figure 2. Current density versus voltage characteristics for electron only devices of the organic semiconductor PNDI(2OD)-2T, with a TPBi interlayer either thermally evaporated (black empty circles) or spin coated from ethanol solution (green filled circles), with an evaporated TPBi interlayer with Ba(5 nm)/Al(100 nm) on top (purple circles), with only a barium (5 nm) interlayer (blue circles), with only a lithium fluoride (1 nm) interlayer (ocher circles) and without interlayer (red circles).

an energetic barrier for charge injection (Supporting Information). In the case of a TPBi interlayer, reducing the metal work function with an additional barium interlayer (TPBi/Ba/Al) does not further improve the current, showing that Fermi-level alignment is already achieved with a TPBi/Al contact.

It is further noted that the current in reverse bias, corresponding to electron injection from the aluminum bottom electrode, remains comparable for all devices. The injected current from the plain aluminum top electrode (forward bias) is lower in comparison, which may have several potential origins, such as damage of the top surface of the organic semiconductor or the presence of different interface dipoles formed at the bottom and top electrode, for instance due to an oxide layer at the surface of the bottom electrode.^[2,15]

To confirm that the deposition method of the interlayer does not have a significant influence on the morphology, AFM micrographs of the surface of both films were taken (Figure 3). In Figure 3a, the surface of the spin-coated TPBi film is shown and in Figure 3b the evaporated TPBi film as a reference, both on top of the polymer layer. The root-mean-square (RMS) roughness for the evaporated film is 1.87 ± 0.18 nm, compared with 1.33 ± 0.12 nm for the spin-coated film. This shows that equally smooth films can be obtained by spin coating of the interlayer as compared with evaporated layers. From the associated AFM phase images shown in Figure S2 (Supporting Information), it is observed that for both deposition methods, a continuous TPBi film is obtained, although it appears that a certain degree of molecular organization is obtained for the spin-coated film. For the layer stack with the spin-coated interlayer, a total thickness (including the polymer layer) of 131 ± 1.4 nm was determined, and 131 ± 3.1 nm for the layer stack with evaporated TPBi. The thickness of the pure PNDI(2OD)-2T film was measured to be 127 nm, confirming that in both cases, a TPBi

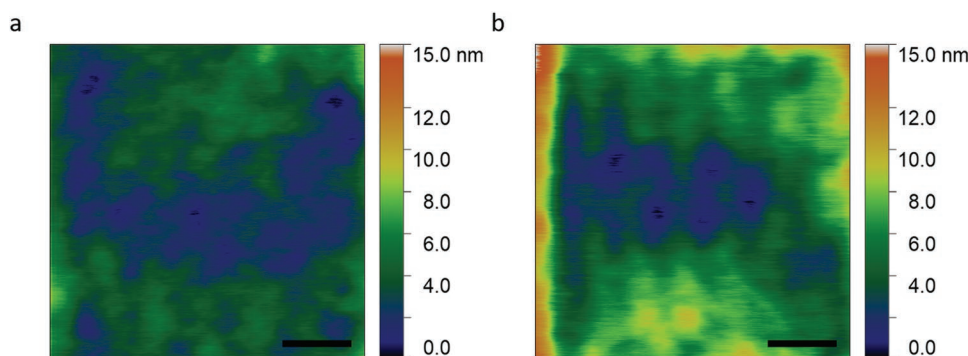


Figure 3. AFM images for TPBi deposited on top of PNDI(2OD)-2T via: a) spin coating, and b) thermal evaporation. The scale bar is 2 μm .

interlayer of 4 nm was present and that the polymer layer thickness remains unaffected by spin coating the interlayer on top.

To assess whether the use of a TPBi interlayer yields an ohmic electron contact, we investigate whether the injected current is space-charge limited. For ohmic injection, the magnitude of the space-charge-limited electron current will be determined by the electron mobility of PNDI(2OD)-2T, according to the Mott–Gurney square law:^[16]

$$J = \frac{9}{8} \varepsilon \mu \frac{V^2}{L^3} \quad (1)$$

where ε is the permittivity, μ the charge-carrier mobility, and L the layer thickness. Fitting the measured electron current with Equation 1 yields a mobility of $5 \times 10^{-8} \text{ m}^2 \text{ V}^{-1} \text{ s}^{-1}$. This mobility is equal to the value determined previously for this polymer,^[11] indicating that the current is indeed bulk limited and thus the electron contact can be considered ohmic, even without the use of reactive metals.^[8]

For a more detailed analysis, temperature-dependent J – V curves were measured, as displayed in **Figure 4**. Subsequently, the experimental data were fitted with a numerical drift-diffusion model. This model includes a charge-carrier mobility that is dependent on the electric field, charge-carrier density, and temperature according to the extended Gaussian disorder model (EGDM).^[17] The temperature dependence of the

J – V characteristics is mainly governed by the energetic disorder of the polymer. As observed in **Figure 4**, a decrease in current of about one order of magnitude is observed by going from 295 to 215 K for both deposition methods of the interlayer. Applying the EGDM, this temperature dependence corresponds to an energetic disorder σ of 0.09 eV, as obtained previously for electron transport in this polymer.^[14] We note that it is possible to model the devices from both interlayer deposition methods using the same parameters. No electron trapping was included, which can be expected considering the LUMO energy of PNDI(2OD)-2T is situated inside the trap-free window.^[18] From these simulations, a room-temperature electron mobility of $2 \times 10^{-8} \text{ m}^2 \text{ V}^{-1} \text{ s}^{-1}$ was determined, which is slightly lower than the mobility obtained by Equation 1, since the mobility in the simulation is extrapolated to zero charge-carrier density and electric field. Overall, the simulations show that the current density is indeed governed by the electron-transport properties of PNDI(2OD)-2T and therefore not limited by an injection barrier.

To investigate if the application of a tunneling interlayer for electron injection can be generalized to more materials, we also apply interlayers of bathocuproine (BCP) and 1,3,5-tri(m-pyridin-3-ylphenyl)benzene (TmPyPB) by means of thermal evaporation or spin coating from ethanol solution. These materials are commonly used as electron-transport materials and have electron affinities significantly lower than PNDI(2OD)-2T, which is the expected main requirement for their use as thin

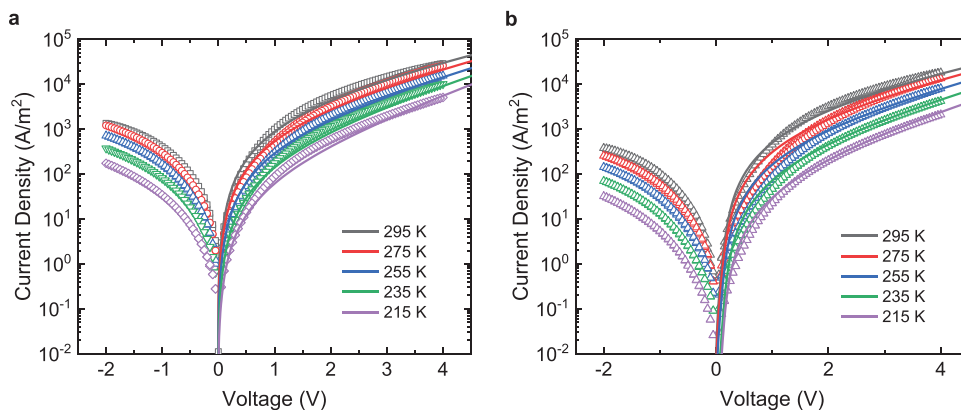


Figure 4. Temperature-dependent J – V characteristics for electron-only devices of PNDI(2OD)-2T with TPBi interlayers that were either: a) evaporated or b) spin coated. Symbols represent the measured data, the solid lines show the drift-diffusion simulations using the EGDM combined with ohmic injecting contacts. The film thicknesses of the PNDI(2OD)-2T layers equal 119 nm (a) and 129 nm (b).

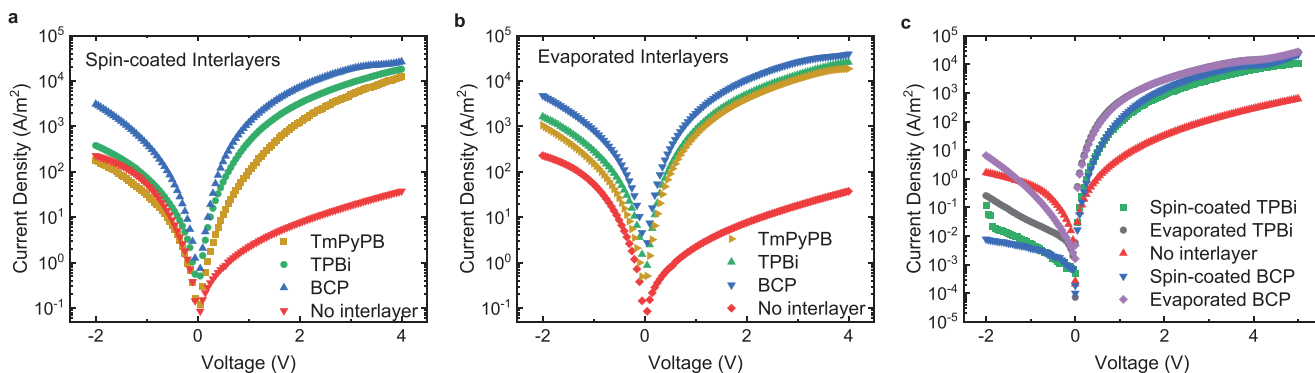


Figure 5. J - V characteristics of electron-only devices of PNDI(2OD)-T2 employing different interlayer materials applied by: a) spin coating or b) thermal evaporation. c) J - V characteristics of electron-only devices of the organic semiconductor IT-4F with different interlayer materials and different deposition methods. In all cases, application of an interlayer substantially improves the injected electron current in IT-4F.

interlayers for electron injection. The BCP and TmPyPB interlayers were all spin coated with the same recipe as for TPBi. In **Figure 5a,b**, the J - V curves of devices with the different interlayer materials are shown. It is observed that the current density significantly increases upon application of all interlayers, where the obtained J - V curves of the devices with the various interlayers are all fairly similar. It should be noted that with the spin-coated interlayer of TmPyPB, a slightly lower electron current is obtained, which may be do suboptimal film formation. The results for an evaporated TmPyPB layer show that efficient electron injection is achievable also with this interlayer material. With both spin-coated an evaporated BCP, an even slightly higher current is observed compared with a TPBi interlayer. The current in reverse bias, corresponding to electron injection from the aluminum bottom electrode, also seems to be enhanced, potentially indicating diffusion of the small BCP molecules into the layer. However, this observation is not fully understood. Overall, the improved injected current by the application of organic interlayers with a low electron affinity indicates that this strategy can be generalized to more materials.

After having confirmed that the presented injection strategy is not limited to a single interlayer material, we proceed with substituting the organic semiconductor in which electrons are to be injected. To this end, we chose the non-fullerene acceptor material 3,9-bis(2-methylene-((3-(1,1-dicyanomethylene)-6,7-difluoro)-indanone))-5,5,11,11-tetrakis(4-hexylphenyl)-dithieno[2,3-d:2',3'-d']-s-indaceno[1,2-b:5,6-b']dithiophene (IT-4F), which finds application in efficient organic solar cells.^[19] IT-4F as opposed to the polymer PNDI(2OD)-2T is a small molecule, which is expected to render solution processing of the interlayer on top more challenging because of both mechanical properties and solubility. However, as displayed in **Figure 5c**, the J - V curves of electron-only devices of IT-4F yield similar improvements upon application of either evaporated, or spin-coated interlayers. Moreover, also for IT-4F both TPBi and BCP interlayers give similar results, improving the injected electron current by about two orders of magnitude compared with a bare aluminum electrode. These measurements demonstrate that a tunneling interlayer may also improve the electron contact in solar cells based on non-fullerene acceptors, not requiring the use of instable reactive metals, while also being conveniently compatible with solution processing.

3. Conclusion

In summary, we have shown that adding a thin-organic tunneling interlayer can be used to obtain an ohmic electron contact on organic semiconductors. The main requirement for this interlayer is that the material has a lower electron affinity than the organic semiconductor in which the charge is injected. It was demonstrated that with the help of such an interlayer, ohmic electron injection can be achieved even from a plain aluminum electrode, whereas the conventional method of using low work-function reactive metals without interlayers results in injection barriers. In addition, we also showed that these interlayers can be solution processed on top of organic-semiconductor layers, as demonstrated for the polymer PNDI(2OD)-2T as well as for the non-fullerene acceptor IT-4F. These results show that the use of such interlayers results in superior electron injection compared with reactive metals and are even compatible with solution processing.

4. Experimental Section

Materials: All materials were used as received without further purification. Poly((*N,N'*-bis(2-octyloxy)naphthalene-1,4,5,8-bis(dicarboximide)-2,6-diyl)-alt-5,5'-(2,2'-bithiophene)) PNDI(2OD)-2T, 2,2',2''-(1,3,5-Benzotriyl)-tris(1-phenyl-1-H-benzimidazole) (TPBi), bathocuproine (BCP), 1,3,5-tri(m-pyridin-3-ylphenyl)benzene (TmPyPB), and 3,9-bis(2-methylene-((3-(1,1-dicyanomethylene)-6,7-difluoro)-indanone))-5,5,11,11-tetrakis(4-hexylphenyl)-dithieno[2,3-d:2',3'-d']-s-indaceno[1,2-b:5,6-b']dithiophene (IT-4F) were purchased from Ossilia Ltd. Dried ethanol was purchased from Merck KGaA.

Device Fabrication: The organic semiconductors PNDI(2OD)-2T and IT-4F were dissolved in chlorobenzene with a concentration of 10 mg mL⁻¹ for PNDI(2OD)-2T and 20 mg mL⁻¹ for IT-4F, respectively. The solutions were stirred for 18 h at 60 °C. The interlayer materials TPBi, BCP, and TmPyPB were dissolved in dry ethanol with a concentration of 0.5 mg mL⁻¹ each and stirred for 18 h at room temperature. Glass substrates were washed with soap, followed by ultrasonic cleaning with acetone and isopropanol, and UV-ozone treatment. All subsequent device fabrication and electrical characterization steps were performed in controlled nitrogen atmosphere. A 30-nm aluminum bottom electrode was thermally evaporated in high vacuum at a base pressure of 1 × 10⁻⁶ mbar. The organic semiconductors were spin coated with a speed of 1000 rpm for 60 s, followed by 30 s at 4000 rpm. The solution-processed interlayers were spin coated on top of the organic-semiconductor layers at 3000 rpm for 60 s. For the evaporated

interlayers, thermal evaporation was carried out in high vacuum at a base pressure of 2×10^{-6} mbar. The devices were completed with a thermally evaporated aluminum top electrode with a thickness of 100 nm.

Device Characterization: All electrical measurements were performed inside a nitrogen-filled glovebox with a Keithley 2400 source meter. Layer thicknesses were measured with a DektakXT profilometer. AFM measurements were performed with a Dimension 3100 AFM.

Supporting Information

Supporting Information is available from the Wiley Online Library or from the author.

Acknowledgements

Open access funding enabled and organized by Projekt DEAL.

Conflict of Interest

The authors declare no conflict of interest.

Data Availability Statement

The data that support the findings of this study are available from the corresponding author upon reasonable request.

Keywords

charge injection, charge transport, organic electronic devices, organic semiconductors

Received: December 1, 2022

Revised: January 18, 2023

Published online: March 22, 2023

- [1] P. W. M. Blom, *Adv. Mater. Technol.* **2020**, *5*, 2000144.
- [2] Y. Shen, A. R. Hosseini, M. H. Wong, G. G. Malliaras, *ChemPhysChem* **2004**, *5*, 16.
- [3] R. H. Friend, R. W. Gymer, A. B. Holmes, J. H. Burroughes, R. N. Marks, C. Taliani, D. D. C. Bradley, D. A. Dos Santos, J. L. Bredas, M. Lögdlund, W. R. Salaneck, *Nature* **1999**, *397*, 121.
- [4] B. F. Bory, P. R. F. Rocha, R. A. J. Janssen, H. L. Gomes, D. M. De Leeuw, S. C. J. Meskers, *Appl. Phys. Lett.* **2014**, *105*, 123302.
- [5] M. Kröger, S. Hamwi, J. Meyer, T. Riedl, W. Kowalsky, A. Kahn, *Org. Electron.* **2009**, *10*, 932.
- [6] M. Kröger, S. Hamwi, J. Meyer, T. Riedl, W. Kowalsky, A. Kahn, *Appl. Phys. Lett.* **2009**, *95*, 123301.
- [7] N. B. Kotadiya, H. Lu, A. Mondal, Y. Ie, D. Andrienko, P. W. M. Blom, G. A. H. Wetzelaer, *Nat. Mater.* **2018**, *17*, 329.
- [8] R. Steyrlleuthner, M. Schubert, F. Jaiser, J. C. Blakesley, Z. Chen, A. Facchetti, D. Neher, *Adv. Mater.* **2010**, *22*, 2799.
- [9] J. Hwang, A. Wan, A. Kahn, *Mater. Sci. Eng.: R. Rep.* **2009**, *64*, 1.
- [10] H. Vázquez, R. Oszwaldowski, P. Pou, J. Ortega, R. Pérez, F. Flores, A. Kahn, *Europhys. Lett.* **2004**, *65*, 802.
- [11] N. B. Kotadiya, P. W. M. Blom, G.-J. A. H. Wetzelaer, *Nat. Photonics* **2019**, *13*, 765.
- [12] K. Zhang, N. B. Kotadiya, X. Y. Wang, G. J. A. H. Wetzelaer, T. Marszalek, W. Pisula, P. W. M. Blom, *Adv. Electron. Mater.* **2020**, *6*, 1901352.
- [13] L. Gao, Z. G. Zhang, L. Xue, J. Min, J. Zhang, Z. Wei, Y. Li, *Adv. Mater.* **2016**, *28*, 1884.
- [14] G.-J. A. H. Wetzelaer, M. Kuik, Y. Olivier, V. Lemaire, J. Cornil, S. Fabiano, M. A. Loi, P. W. M. Blom, *Phys. Rev. B* **2012**, *86*, 165203.
- [15] A. Ioannidis, J. S. Facci, M. A. Abkowitz, *J. Appl. Phys.* **1998**, *84*, 1439.
- [16] J. A. Rohr, D. Moia, S. A. Haque, T. Kirchartz, J. Nelson, *J. Phys. Condens. Matter* **2018**, *30*, 105901.
- [17] W. F. Pasveer, J. Cottaar, C. Tanase, R. Coehoorn, P. A. Bobbert, P. W. Blom, D. M. de Leeuw, M. A. Michels, *Phys. Rev. Lett.* **2005**, *94*, 206601.
- [18] N. B. Kotadiya, A. Mondal, P. W. M. Blom, D. Andrienko, G. A. H. Wetzelaer, *Nat. Mater.* **2019**, *18*, 1182.
- [19] J. Hou, O. Inrganas, R. H. Friend, F. Gao, *Nat. Mater.* **2018**, *17*, 119.